

Synthesis and Structure of Complex Salts with 3-Arylidene-1-pyrrolinium Cations

J. K. Voronina^{a, *}, E. N. Zorina-Tikhonova^a, D. O. Blinou^a, O. V. Zvereva^{a, b}, E. Yu. Peshkova^{a, c},
A. V. Smolobochkin^d, and I. L. Eremenko^{a, e}

^a Kurnakov Institute of General and Inorganic Chemistry, Russian Academy of Sciences, Moscow, 119991 Russia

^b National Research University, Higher School of Economics, Moscow, 101000 Russia

^c Moscow South-Eastern School Named after V.I. Chuikov, Moscow, Russia

^d Arbuzov Institute of Organic and Physical Chemistry, Federal Research Center Kazan Scientific Center, Russian Academy of Sciences, Kazan, 420088 Russia

^e Nesmeyanov Institute of Organoelement Compounds, Russian Academy of Sciences, Moscow, 119334 Russia

*e-mail: julavoronina@mail.ru

Received May 13, 2022; revised May 27, 2022; accepted May 30, 2022

Abstract—The complex salts (R-BpH)[MAn_x]⁺, where R-BpH is the protonated 3-arylidene-1-pyrrolinium cation, An is the chloride, nitrate, or dimethylmalonate anion, were synthesized by reactions of 3-arylidene-1-pyrrolinium trifluoroacetates with zinc(II) chloride, copper(II) nitrate, and iron(III) chloride or iron(III) dimethylmalonate. All products were characterized by IR spectroscopy and X-ray diffraction (CCDC nos. 2169556–2169560). It was shown that all crystal structures are formed by classical N–H...O and O–H...O type hydrogen bonds between the complex anions and the protonated organic molecules and by π...π contacts between the latter.

Keywords: complex salt, 3-arylidene-1-pyrrolidine, X-ray diffraction, structure of the complex salt, non-cova-lent interactions, zinc(II) chloride, copper(II) nitrate, iron(III) chloride, iron(III) dimethylmalonate, dicarboxylates

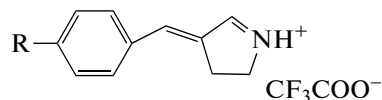
DOI: 10.1134/S107032842270018X

INTRODUCTION

A highly relevant research area of the modern chemistry is the synthesis of new coordination compounds with specified properties based on the combination of organic and inorganic blocks that possess known properties. By varying the types, the ratio, and the mutual orientation of these blocks in molecules, it is possible to control the properties of the final compounds [1–3]. In particular, this approach was used to obtain polyfunctional materials exhibiting both magnetic and optical behavior or optical behavior and biological activity [1, 4, 5]. Previously, a number of quinolinium, isoquinolinium, and pyridinium halometallate complexes have been studied [6–10]. Pyrroline and pyrrolidine derivatives, that is, five-membered heterocyclic compounds containing a nucleophilic nitrogen atom, are among the most naturally abundant (nicotine, proline) [11–16] and most promising synthetic biologically active products [17–20]. Besides, the large number of reaction sites makes these compounds convenient precursors for the preparation of more complex organic cages [20–25]. Coordination compounds of essential metals with pyrroline derivatives are of interest as not only potential biologically

active compound, but also as precursors for the subsequent post-synthetic modification of the obtained complexes.

This study is devoted to the synthesis and structural investigation of complex salts of iron(III) (**I**, **II**), copper(II) (**III**), and zinc (**IV**, **V**) with 3-arylidene-1-pyrrolinium cations. The structural formula of 3-arylidene-1-pyrrolidine derivatives used in the reactions is shown in Scheme 1.



R = Cl (for **I** and **III**), OH (for **II** and **IV**), OEt (for **V**)
Scheme 1.

EXPERIMENTAL

The compounds were synthesized in air using distilled water and the following commercial reagents and solvents: chloroform (CHCl₃, reagent grade, Khimmed), FeCl₃·6H₂O (reagent grade, Reakhim), Fe₂(SO₄)₃·9H₂O (reagent grade, Reakhim), Ba(OH)₂

8H₂O (reagent grade, Reakhim), Cu(NO₃)₂·3H₂O (98%, Roth), ZnCl₂·xH₂O (>99%, Alfa Aesar), dimethylmalonic acid (H₂Me₂Mal, Fluorochem). The compounds (*p*-Cl-BpH)CF₃CO₂, (*p*-OH-BpH)CF₃CO₂, (*p*-OEt-BpH)CF₃CO₂, and *p*-OH-Bp were prepared by a previously reported procedure [25].

Infrared spectra of the products were measured on a Perkin Elmer Spectrum 65 spectrometer equipped with a Quest ATR Accessory attachment (Specac) by the attenuated total reflectance (ATR) method in the 400–4000 cm⁻¹ range.

Single crystal X-ray diffraction study of the compounds was carried out on a Bruker D8 Venture automated diffractometer equipped with a CCD array detector (graphite monochromator, λ MoK_α = 0.71073 Å, ω - and φ -scan mode) at a temperature of 100 K. Semi-empirical absorption corrections were applied using the SADABS program [26]. The structures were solved by direct methods using the SHELXT 2014/4 software [27] and refined, first, in the isotropic and then in the anisotropic approximation using the SHELXL-2018/3 software [28] and OLEX2 [29]. The hydrogen atoms of the NH and OH groups in all compounds, except for the disordered moieties of **II**, were identified using the difference electron density maps; the other atoms were placed into the geometrically calculated positions and included in the refinement in the riding model. The crystallographic parameters and structure refinement details are summarized in Table 1.

The full set of X-ray diffraction parameters of complexes **I**–**V** is deposited with the Cambridge Crystallographic Data Centre (CCDC nos. 2169556–2169560) and is available from deposit@ccdc.cam.ac.uk or http://www.ccdc.cam.ac.uk/data_request/cif.

The geometry of the metal polyhedra was determined using the SHAPE 2.1 software package [30].

Synthesis of (*p*-Cl-BpH)₂[FeCl₄](CF₃COO) (I**).** A weighed amount of FeCl₃·6H₂O (0.0152 g, 0.057 mmol) was dissolved in CHCl₃ (10 mL), and then (*p*-Cl-BpH)CF₃COO (0.0339 g, 0.111 mmol) was added to the solution. As this took place, the solution color changed from yellow to red. The reaction mixture was stirred for 60 min at room temperature (20°C), filtered, and allowed to slowly evaporate in air. After 3 days, dark red crystals suitable for X-ray diffraction were formed. The yield was 0.01 g (25% based on the initial amount of iron(III)).

IR (ATR; ν , cm⁻¹): 3268 m, 1911 w, 1628 w, 1576 s, 1488 m, 1444 m, 1376 w, 1304 s, 1234 w, 1192 m, 1162 s, 1085 s, 976 m, 907 s, 882 m, 829 m, 727 s, 492 s.

Synthesis of (*p*-OH-BpH)₃[Fe(Me₂Mal)₃]·2H₂O (II**).** Weighed amounts of Ba(OH)₂·8H₂O (0.0473 g, 0.15 mmol) and H₂Me₂Mal (0.0396 g, 0.3 mmol) were dissolved in water (15 mL). A weighed amount of Fe₂(SO₄)₃·9H₂O (0.0281 g, 0.05 mmol) was added to

the resulting colorless solution, and the solution color changed to pale yellow. The solution was stirred for 45 min at room temperature (20°C) and filtered. A weighed amount of *p*-OH-Bp (0.052 g, 0.3 mmol) was added to the mother liquor with stirring, and the solution color changed to bright yellow. The solution was stirred for 30 min, filtered, and allowed to slowly evaporate in air. After 14 days, crystal suitable for X-ray diffraction were formed. The yield was 0.038 g (44% based on the initial amount of iron(III)).

IR (ATR; ν , cm⁻¹): 3439 w, 3051 m, 2986 m, 2875 m, 2676 m, 1568 s, 1507 s, 1458 s, 1392 s, 1348 s, 1287 s, 1246 s, 1200 s, 1162 s, 1112 s, 976 s, 886 s, 832 s, 759 s, 697 s, 590 s, 538 s, 500 s.

Synthesis of (*p*-Cl-BpH)₄[Cu(NO₃)₄](NO₃)₂ (III**).** Weighed amounts of Cu(NO₃)₂·3H₂O (0.1 g, 0.413 mmol) and (*p*-Cl-BpH)CF₃CO₂ (0.243 g, 0.826 mmol) were dissolved in CHCl₃ (40 mL) on heating (40°C), and the solution was stirred for 1 h, cooled to room temperature, and allowed to slowly evaporate. Approximately 16 days later, blue crystals suitable for X-ray diffraction were formed. The yield was 0.085 g (17% based on the initial amount of copper(II)).

IR (ATR; ν , cm⁻¹): 3220 w, 3142 m, 3064 m, 2979 m, 2891 m, 2841 m, 2786 m, 2647 m, 2085 w, 1891 w, 1748 w, 1660 w, 1634 m, 1612 m, 1584 m, 1562 w, 1491 m, 1464 m, 1437 m, 1423 m, 1381 m, 1306 s, 1286 s, 1197 m, 1185 m, 1169 s, 1121 m, 1088 s, 1038 m, 1008 m, 953 m, 814 s, 786 s, 726 m, 710 m, 699 m, 683 m, 581 m, 526 m, 500 s, 464 m, 426 m, 413 m, 406 m.

Synthesis of (*p*-OH-BpH)₂[ZnCl₄] (IV**).** Weighed amounts of (*p*-OH-BpH)CF₃COO (0.0395 g, 0.144 mmol) and ZnCl₂·xH₂O (0.015 g, 0.072 mmol) were dissolved in ethanol (20 mL). The reaction mixture was stirred with heating (60°C) for 1 h. After a week, crystals suitable for X-ray diffraction were formed. The yield was 0.005 g (12% based on the initial amount of zinc).

Synthesis of (*p*-OEt-BpH)[Zn(H₂O)Cl₃] (V**).** A weighed amount of (*p*-OEt-BpH)CF₃COO (0.0437 g, 0.144 mmol) was dissolved in CHCl₃ (20 mL), and ZnCl₂·xH₂O (0.015 g, 0.072 mmol) was added to the solution. The reaction mixture was stirred for 1 h. The resulting yellow-orange solution was allowed to slowly evaporate. Orange crystals suitable for X-ray diffraction were formed after 11 weeks. The yield was 0.007 g (25% based on the initial amount of copper(II)).

IR (ATR; ν , cm⁻¹): 3226 w, 3085 w, 2986 w, 2936 w, 2888 w, 1890 w, 1772 w, 1683 m, 1574 s, 1512 m, 1444 m, 1383 w, 1306 m, 1258 m, 1194 s, 1155 s, 1039 m, 912 m, 882 w, 840 m, 796 m, 757 s, 725 m, 666 m, 618 m, 586 m, 534 m, 490 s, 406 w.

Table 1. Crystallographic data and structure refinement details for **I–V**

Parameter	Value
Formula	$\text{Cl}_4\text{Fe} \cdot 2(\text{C}_{11}\text{H}_{11}\text{NCl}) \cdot \text{C}_{15}\text{H}_{18}\text{O}_{12}\text{Fe} \cdot 3(\text{C}_{11}\text{H}_{11}\text{NOH}) \cdot 2(\text{H}_2\text{O})$ (I)
<i>M</i>	695.98
System, space group	Triclinic, $P\bar{1}$
<i>a</i> , Å	8.7822(3)
<i>b</i> , Å	11.2645(4)
<i>c</i> , Å	15.7304(6)
α , deg	80.075(1)
β , deg	73.931(1)
γ , deg	73.043(1)
<i>V</i> , Å ³	1423.22(9)
<i>Z</i>	2
μ , mm ⁻¹	1.14
Crystal size, mm	0.12 × 0.11 × 0.05
<i>T</i> _{min} , <i>T</i> _{max}	0.316, 0.381
No. of measured reflections	13522
No. of unique reflections	6842
No. of observed [<i>I</i> > 2 <i>s</i> (<i>I</i>)] reflections	6334
<i>R</i> _{int}	0.017
<i>R</i> ₁ / <i>wR</i> (<i>F</i> ²) (<i>I</i> > 2 <i>s</i> (<i>I</i>))	0.0233/0.0560
<i>R</i> ₁ / <i>wR</i> (<i>F</i> ²) (for all reflections)	0.0259/0.0574
No. of refined parameters	351
Residual electron density (max/min), e Å ⁻³	0.40/−0.31
Polyhedron of the central metal ion (SHAPE 2.1), CShM	Tetrahedron, 0.087
	$\text{Cl}_4\text{Zn} \cdot 2(\text{C}_{11}\text{H}_{11}\text{NOH})$ (IV)
<i>M</i>	1206.23
System, space group	Monoclinic, $C2/c$
<i>a</i> , Å	19.932(4)
<i>b</i> , Å	12.768(2)
<i>c</i> , Å	40.083(8)
α , deg	97.217(5)
β , deg	83.118(2)
γ , deg	88.858(2)
<i>V</i> , Å ³	69.875(2)
<i>Z</i>	1
μ , mm ⁻¹	0.37
Crystal size, mm	0.1 × 0.02 × 0.01
<i>T</i> _{min} , <i>T</i> _{max}	0.290, 0.381
No. of measured reflections	13522
No. of unique reflections	6842
No. of observed [<i>I</i> > 2 <i>s</i> (<i>I</i>)] reflections	6334
<i>R</i> _{int}	0.0185
<i>R</i> ₁ / <i>wR</i> (<i>F</i> ²) (<i>I</i> > 2 <i>s</i> (<i>I</i>))	0.0860/0.1797
<i>R</i> ₁ / <i>wR</i> (<i>F</i> ²) (for all reflections)	0.1924/0.2288
No. of refined parameters	351
Residual electron density (max/min), e Å ⁻³	0.46/−0.57
Polyhedron of the central metal ion (SHAPE 2.1), CShM	Tetrahedron, 0.398
	$\text{Cl}_3\text{H}_2\text{OZn} \cdot \text{C}_{11}\text{H}_{11}\text{NOC}_2\text{H}_5$ (V)
<i>M</i>	392.00
System, space group	Triclinic, $P\bar{1}$
<i>a</i> , Å	17.2976(9)
<i>b</i> , Å	7.6362(4)
<i>c</i> , Å	18.1929(9)
α , deg	102.091(2)
β , deg	109.599(4)
γ , deg	94.456(4)
<i>V</i> , Å ³	69.875(2)
<i>Z</i>	2
μ , mm ⁻¹	0.74
Crystal size, mm	0.18 × 0.16 × 0.12
<i>T</i> _{min} , <i>T</i> _{max}	0.342, 0.381
No. of measured reflections	10076
No. of unique reflections	4887
No. of observed [<i>I</i> > 2 <i>s</i> (<i>I</i>)] reflections	4583
<i>R</i> _{int}	0.019
<i>R</i> ₁ / <i>wR</i> (<i>F</i> ²) (<i>I</i> > 2 <i>s</i> (<i>I</i>))	0.0272/0.0708
<i>R</i> ₁ / <i>wR</i> (<i>F</i> ²) (for all reflections)	0.0290/0.0719
No. of refined parameters	357
Residual electron density (max/min), e Å ⁻³	0.33/−0.40
Polyhedron of the central metal ion (SHAPE 2.1), CShM	Square, 0.017
	Tetrahedron, 0.164
	Tetrahedron, 0.522

Table 2. Selected bond lengths in the complex anions according to X-ray diffraction data

Bond	Length, Å	Bond	Length, Å
I			
Fe(1)–C(11)	2.1786(4)	Fe(1)–Cl(3)	2.1956(4)
Fe(1)–C(12)	2.1924(4)	Fe(1)–Cl(4)	2.2071(4)
II			
Fe(1)–O(1)	1.961(4)	Fe(1)–O(7)	2.003(5)
Fe(1)–O(3)	1.963(5)	Fe(1)–O(9)	2.002(5)
Fe(1)–O(5)	1.991(5)	Fe(1)–O(11)	2.009(5)
III			
Cu(1)–O(4S)	1.9649(12)	Cu(1)–O(7S)	1.9650(13)
Cu(1)–O(4S)	1.9649(12)	Cu(1)–O(7S)	1.9651(13)
IV			
Zn(1)–Cl(1)	2.2797(5)	Zn(1)–Cl(2)	2.2574(5)
Zn(1)–Cl(1)	2.2797(5)	Zn(1)–Cl(2)	2.2574(5)
V			
Zn(1)–Cl(1)	2.2304(5)	Zn(1)–Cl(2)	2.2609(5)
Zn(1)–O(1)	2.0218(14)	Zn(1)–Cl(3)	2.2521(5)

RESULTS AND DISCUSSION

Complex salts **I** and **III**–**V** were prepared by the reactions of 3-arylidenepyrrolinium trifluoroacetate derivatives with iron(III) chloride (**I**), copper(II) nitrate (**III**), and zinc chloride (**IV**, **V**) at M : (R-BpH) CF₃COO ratio of 1 : 2 in chloroform (for **I**, **III**, and **V**) or in ethanol (for **IV**). The reactions gave complex salts containing inorganic complex anions [FeCl₄][–] (**I**), [Cu(NO₃)₄]^{2–} (**III**), [ZnCl₄]^{2–} (**IV**), and [Cu(NO₃)₄]^{2–} (**V**) and organic 3-arylidenepyrrolinium cations (Scheme 1). The replacement of inorganic anions by the dimethylmalonate anion also resulted in the formation of complex salt **II**.

The structure of the products was determined by X-ray diffraction. Protonated 3-arylidenepyrrolinium is present as the cationic part in all complexes. The anionic part in complexes **I** and **III** contains an acid residue, in addition to the complex anion. In **III**, this is a mineral acid anion, while in **I**, it is the trifluoroacetate anion, which is the counter-ion in the initial organic salt. In complexes **II**, **IV**, and **V**, the anionic part is composed of only the complex anion.

In iron(III) complex salts (**I** and **II**), the composition and structure of the complex anion is determined by the nature of the ligand: in the former case, the iron

geometry is a nearly ideal tetrahedron formed upon coordination of four chloride ions (Fig. 1a). The shortest Fe–Cl distance is observed for the Cl(1) atom and the longest distance is that involving the Cl(4) atom (Table 2); this is due to weak non-covalent interactions involving these atoms. It is of interest that strong NH...O hydrogen bonds (Table 3) are formed in the crystal only between the organic cation and trifluoroacetate anion, which gives rise to a nearly planar hydrogen-bonded 2(*p*-Cl-BpH)⁺:CF₃CO₂[–] synthon. The [FeCl₄][–] anion is not only off this plane, but also does not form any non-covalent contacts more significant than CH...Cl. As a result, the molecular packing in the crystals is formed by π ... π contacts between the arylidenepyrroline moieties and by weak CH...O and CH... π contacts and represents an alternation of the anionic layer composed of FeCl₄[–] and CF₃COO[–] species and a cationic layer made of arylidenepyrroline molecules (Fig. 1b).

The anion structure in compound **II** is similar to the structure of tris-malonate ferrates prepared earlier [31, 32]. The dimethylmalonate group coordinated to the O(1) and O(3) atoms is located at the shortest distance from iron, while that coordinated to O(9) and O(11) is at the longest distance from iron (Fig. 2a,

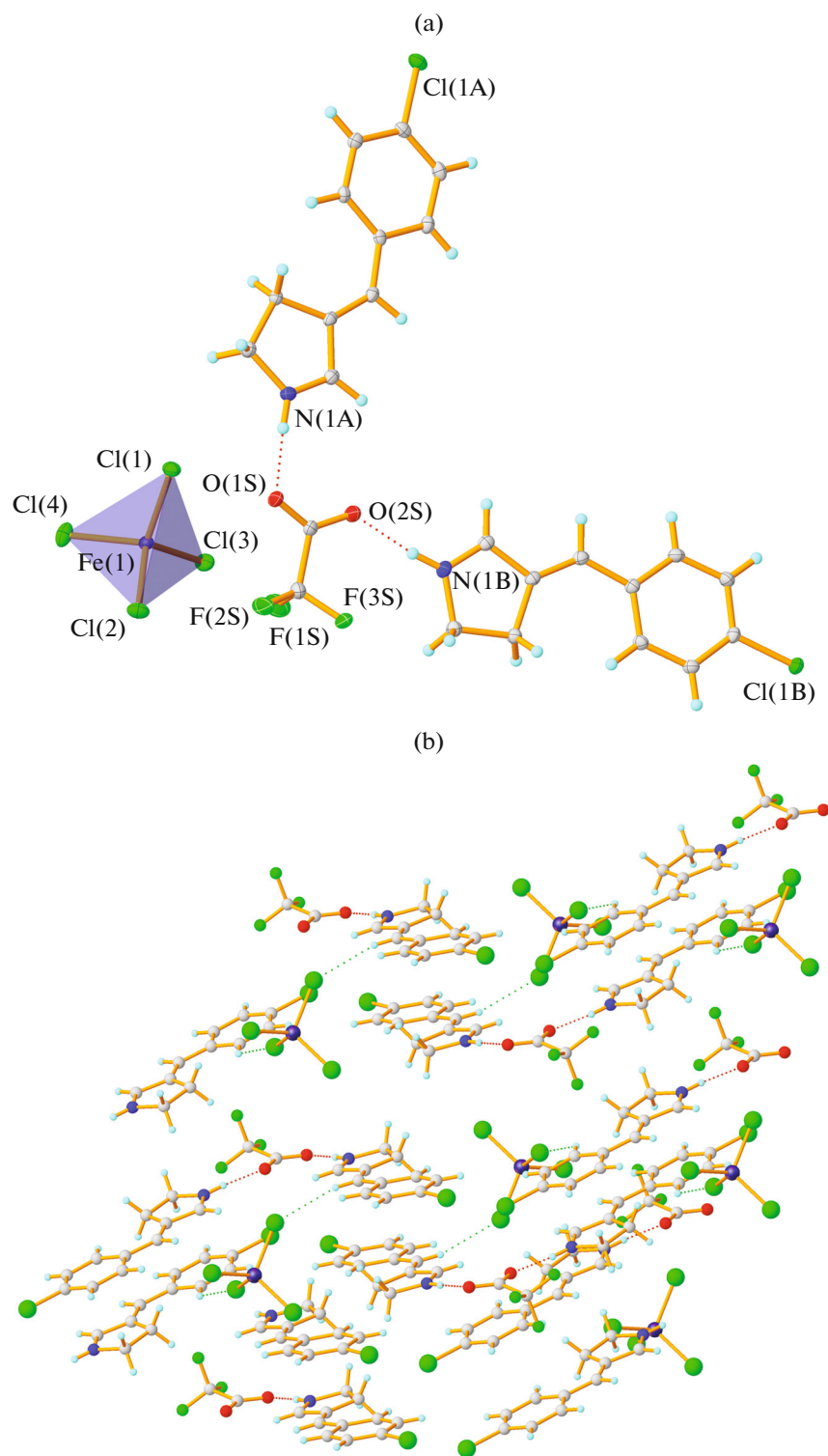


Fig. 1. (a) Structure of complex salt **I** in the crystal; (b) fragment of the crystal packing of **I**. Here and in other figures, ellipsoids are drawn at 50% probability level.

Table 2). Particularly these two groups participate in hydrogen bonding with solvate water molecules. These hydrogen bonds form the principal packing

motif of the crystal (Table 3). The cationic part of the compound is composed of three protonated 3-arylidene-1-pyrrolidine molecules containing a *para*-

Table 3. Geometric parameters of hydrogen bonds in the crystals of compounds I–V

D–H...A	Symmetry code	Distance, Å			D–H...A angle, deg
		D–H	H...A	D...A	
I					
N(1A)–H(1A)...O(1S)	x, y, z	0.85(2)	1.83(2)	2.6783(17)	177(2)
N(1B)–H(1B)...O(2S)	x, y, z	0.88(2)	1.80(2)	2.6744(16)	174(2)
C(5A)–H(5AA)...O(1S)	$2-x, 1-y, 2-z$	0.99	2.48	3.4685(18)	175
C(6A)–H(6A)...Cl(4)	$x, 1+y, z$	0.95	2.74	3.6649(14)	166
C(8B)–H(8B)...Cl(2)	$3-x, 1-y, 1-z$	0.95	2.74	3.4875(15)	136
C(9A)–H(9A)...O(1S)	$-1+x, 1+y, z$	0.95	2.49	3.4004(16)	161
II					
N(1A)–H(1A)...O(8)	$1-x, -y, 1-z$	0.88(8)	1.84(8)	2.686(10)	160(8)
N(1B)–H(1B)...O(4)	$x, 1+y, z$	0.84(8)	2.13(8)	2.860(8)	146(7)
O(13')–H(13')...O(5)	$x, 1+y, z$	0.84	1.98	2.818(15)	172
O(13')–H(13')...O(6)	$x, 1+y, z$	0.84	2.55	3.015(16)	116
O(13A)–H(13A)...O(9)	x, y, z	1.06(7)	2.56(6)	3.198(7)	118(4)
O(13A)–H(13A)...O(10)	x, y, z	1.06(7)	1.64(7)	2.696(7)	174(4)
O(13B)–H(13B)...O(12)	x, y, z	0.76(6)	1.87(6)	2.609(6)	165(7)
O(1S)–H(1SA)...O(2)	$-1/2+x, -1/2+y, z$	0.87	1.82	2.691(7)	177
O(1S)–H(1SB)...O(10)	x, y, z	0.87	1.94	2.791(7)	164
O(2S)–H(2SA)...O(7)	x, y, z	0.87	2.52	2.980(7)	114
O(2S)–H(2SA)...O(8)	x, y, z	0.87	2.09	2.945(9)	167
O(2S)–H(2SB)...O(1S)	x, y, z	0.87	1.78	2.656(7)	179
N(1C')–H(1C')...O(2S)	x, y, z	0.88	2.37	2.67(2)	100
N(1C')–H(1C')...O(13B)	x, y, z	0.88	2.51	3.23(3)	139
C(2A)–H(2A)...O(6)	x, y, z	0.95	2.27	3.124(10)	148
C(2B)–H(2B)...O(3)	$x, 1+y, z$	0.95	2.28	3.086(8)	142
C(5)–H(5A)...O(11)	x, y, z	0.98	2.47	3.403(7)	158
C(5)–H(5B)...O(12)	$1-x, y, 1/2-z$	0.98	2.56	3.484(8)	158
C(6A)–H(6A)...O(6)	x, y, z	0.95	2.45	3.322(10)	153
C(9)–H(9A)...O(1)	x, y, z	0.98	2.42	3.352(9)	159
C(9B)–H(9BA)...O(4)	$-1/2+x, 1/2+y, z$	0.95	2.43	3.329(9)	157
C(11')–H(11')...O(2S)	$1/2+x, 1/2+y, z$	0.95	2.37	3.299(18)	165
C(12')–H(12')...O(2)	x, y, z	0.95	2.55	3.464(18)	161
C(14)–H(14A)...O(3)	x, y, z	0.98	2.49	3.440(8)	164
C(5C')–H(5CD)...O(4)	$-1/2+x, 1/2+y, z$	0.99	2.49	3.47(3)	172
C(2C')–H(2C')...O(7)	x, y, z	1.14(12)	2.30(12)	3.05(2)	121(8)
C2(C')–H(2C')...O(11)	x, y, z	1.14(12)	2.54(12)	3.62(2)	157(9)
III					
N(1A)–H(1A)...O(3S)	x, y, z	0.83(2)	1.96(2)	2.7772(18)	173.0(19)
N(1B)–H(1B)...O(2S)	x, y, z	0.87(2)	1.88(2)	2.7443(18)	174(2)
N(1B)–H(1B)...O(3S)	x, y, z	0.87(2)	2.52(2)	3.0488(18)	120.4(16)
C(4A)–H(4AA)...O(8S)	$1-x, 2-y, 1-z$	0.99	2.53	3.240(2)	128
C(2A)–H(2A)...O(1S)	x, y, z	0.95	2.51	3.105(2)	121
C(2B)–H(2B)...O(3S)	x, y, z	0.95	2.47	3.040(2)	118
C(2B)–H(2B)...O(6S)	x, y, z	0.95	2.38	3.288(2)	160
C(8B)–H(8B)...O(8S)	x, y, z	0.95	2.57	3.270(2)	131
C(11B)–H(11B)...Cl(13)	$-1+x, -1+y, -1+z$	0.95	2.80	3.6548(17)	151
C(12A)–H(12A)...O(2S)	$1-x, 1-y, 2-z$	0.95	2.55	3.318(2)	138
IV					
N(1)–H(1)...Cl(1)	$3/2-x, 3/2-y, 1-z$	0.93(3)	2.33(3)	3.2120(16)	158(3)
O(13)–H(13)...C(12)	x, y, z	0.76(3)	2.43(3)	3.1882(17)	177(3)
C(2)–H(2)...O(13)	$x, 1-y, -1/2+z$	0.95	2.27	3.206(2)	169
C(6)–H(6)...Cl(1)	$x, 1-y, -1/2+z$	0.95	2.79	3.6951(19)	160
C(8)–H(8)...Cl(1)	$x, 1-y, -1/2+z$	0.95	2.76	3.6588(18)	158
V					
N(1)–H(1)...Cl(3)	x, y, z	0.81(2)	2.50(2)	3.2296(17)	150(2)
N(1)–H(1)...Cl(3)	$-1-x, 1-y, -z$	0.81(2)	2.81(2)	3.3534(16)	126.4(19)'
O(1)–H(1A)...Cl(1)	$-1+x, y, z$	0.84(3)	2.29(3)	3.0794(17)	157(3)
O(1)–H(1B)...Cl(2)	$-1+x, y, z$	0.82(3)	2.39(3)	3.1640(17)	157(3)
C(5)–H(5B)...Cl(1)	$-x, 1-y, -z$	0.99	2.81	3.6780(19)	146
C(9)–H(9)...O(13)	$3-x, 2-y, 1-z$	0.95	2.56	3.513(2)	178

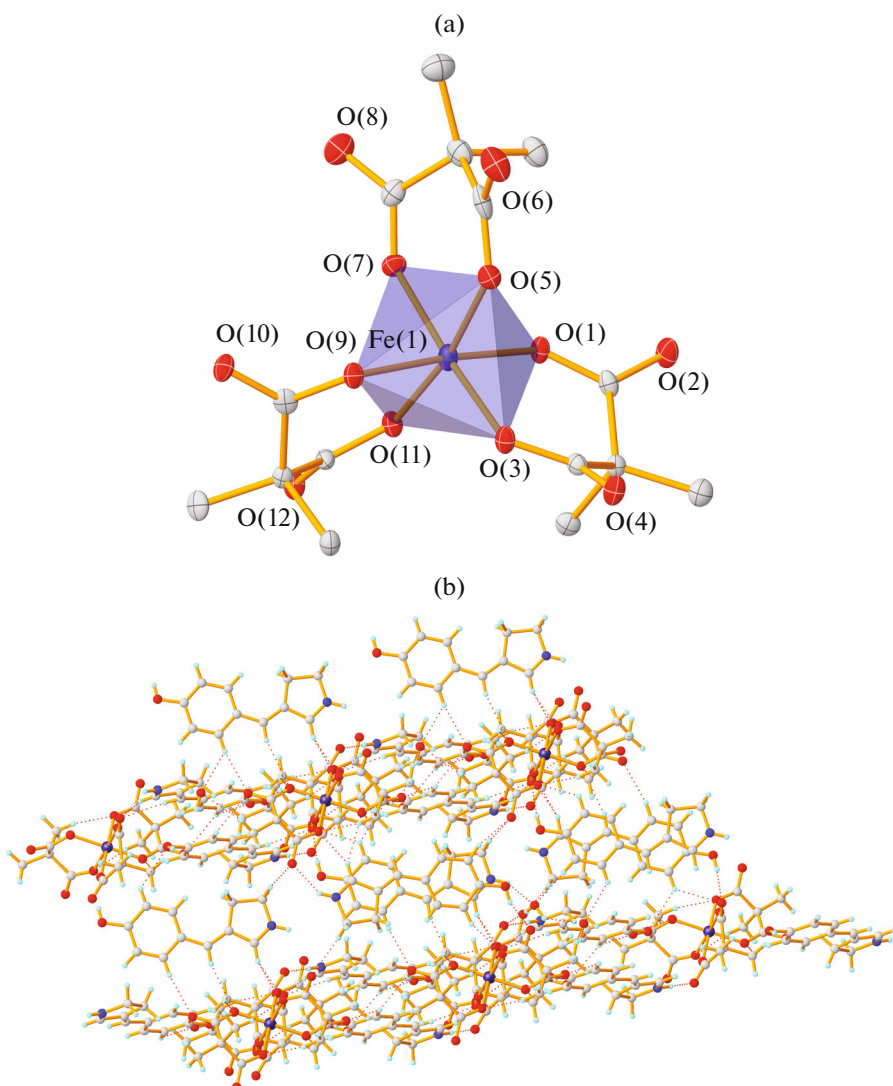


Fig. 2. (a) Structure of the iron tris-dimethylmalonate anion in compound **II**; (b) fragment of the crystal packing of **II**.

hydroxyl group. Thus, the independent part of the unit cell consists of a tris-dimethylmalonate ferrate and arylidenepyrroline stacking dimer, which are located parallel to each other, with the third arylidenepyrroline molecule being located below this plane. Owing to the large number of hydrogen bonding sites, this moiety not only is very stable, but also forms numerous hydrogen bonds (Table 3), giving rise to layers of alternating chains of tris-malonate anions and arylidenepyrroline stacking dimers. The layers are linked via the third arylidenepyrroline moiety. Thus, double layers connected by van der Waals contacts are formed (Fig. 2b).

In compound **III**, the anionic part is represented by nitrate and tetranitrocuprate anions, and the cationic part is formed by protonated 3-arylidene-1-pyrroline with *para*-chlorine atom. The copper atom is located at the center of symmetry in a square planar configu-

ration with nearly equal distances to the oxygen atoms of the coordinated nitro groups (Table 2). The structure of the main synthon is similar to that described for compound **I**; the moiety composed of two organic cations and one nitrate anion is nearly planar, and the independent part of the cuprate anion deviates from the plane (Fig. 3a). Classical NH...O hydrogen bonds are formed between the nitrate and arylidenepyrrolines; the metal-containing anion is connected to the rest of the crystal by weaker CH...O interactions (Table 3). The molecules are packed in the crystal as infinite planar layers connected into a three-dimensional framework by bulky metal-containing anions (Fig. 3b).

In compounds **IV** and **V** zinc chloride acts as a metal-containing anion. The tetrahedral configuration is formed by four chloride anions in compound **IV** (Fig. 4a) and three chloride anions and one water mol-

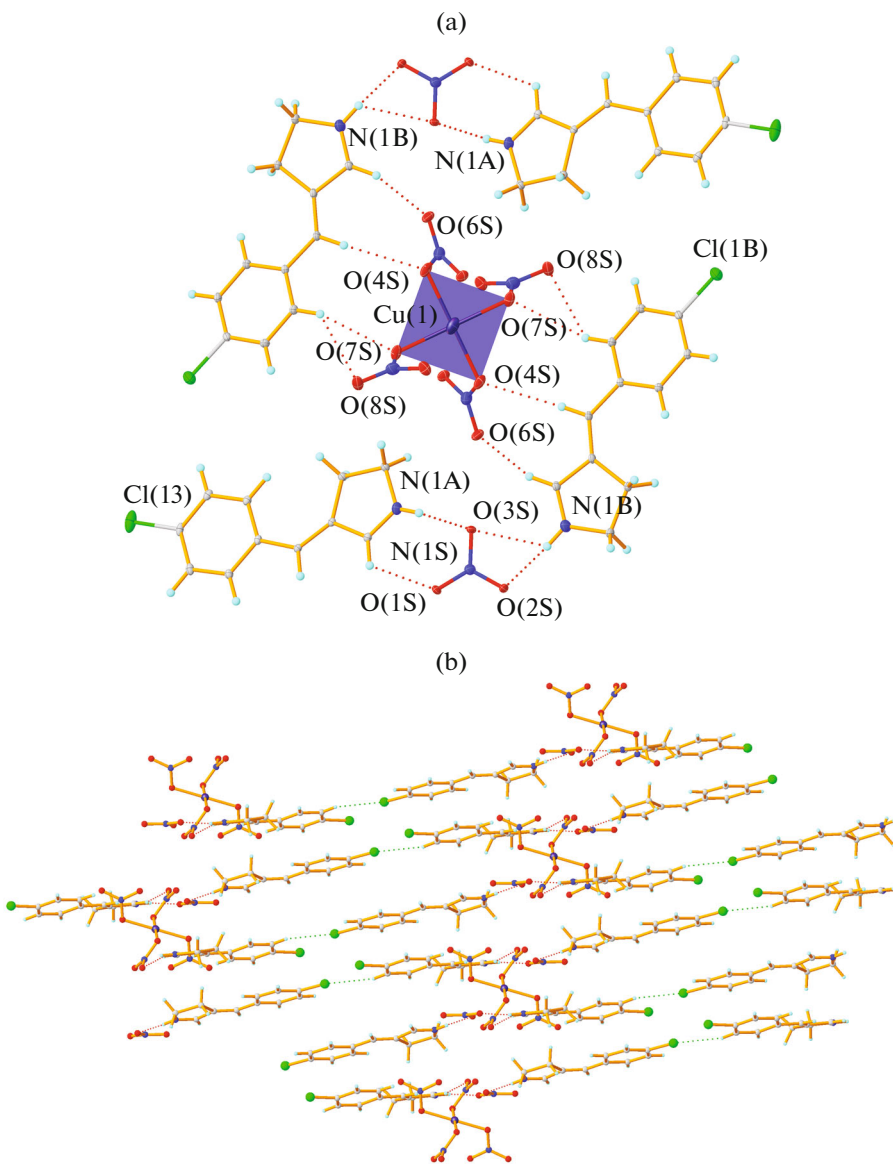


Fig. 3. (a) Structure of complex salt III and hydrogen bonds between the ligands; (b) fragment of the crystal packing of III.

ecule in compound **V** (Fig. 5a). The distances to chlorine atoms in **IV** are somewhat different, probably due to participation of chlorine in strong hydrogen bonds of various types (Table 3). The presence of two hydrogen bond donors in the 3-*p*-hydroxyphenyl-1-pyrroline molecule results in linking of four cations to each complex anion, which gives rise to infinite zigzag chains connected into a three-dimensional framework by $\pi\cdots\pi$, $\text{CH}\cdots\text{O}$, and $\text{CH}\cdots\text{Cl}$ contacts (Fig. 4b).

The tetrahedral zinc atom in **V** is markedly more distorted than that in **IV** (0.522 versus 0.164, according to the Shape program) (Fig. 5a); this is due to the fact that one zinc coordination site is occupied by water instead of chlorine. Thus, in the crystal of this com-

pound, hydrogen bond donors are present in both cationic and anionic parts. The cation and anion are linked by $\text{NH}\cdots\text{Cl}$ bonds, which give rise to centrosymmetrical moieties consisting of two cations and two anions and connected into infinite chains via $\text{OH}\cdots\text{Cl}$ hydrogen bonds between the complex anions (Fig. 5b). This gives rise to infinite ribbons connected via stacking interactions between planar head-to-tail arylidenepyrrolinium moieties.

Crystal packing analysis provides the conclusion that the hydrogen bond between the cation NH group and the anion acceptor atom is the principal structure-forming motif in these compounds. Note that comparison of hydrogen bond parameters for the com-

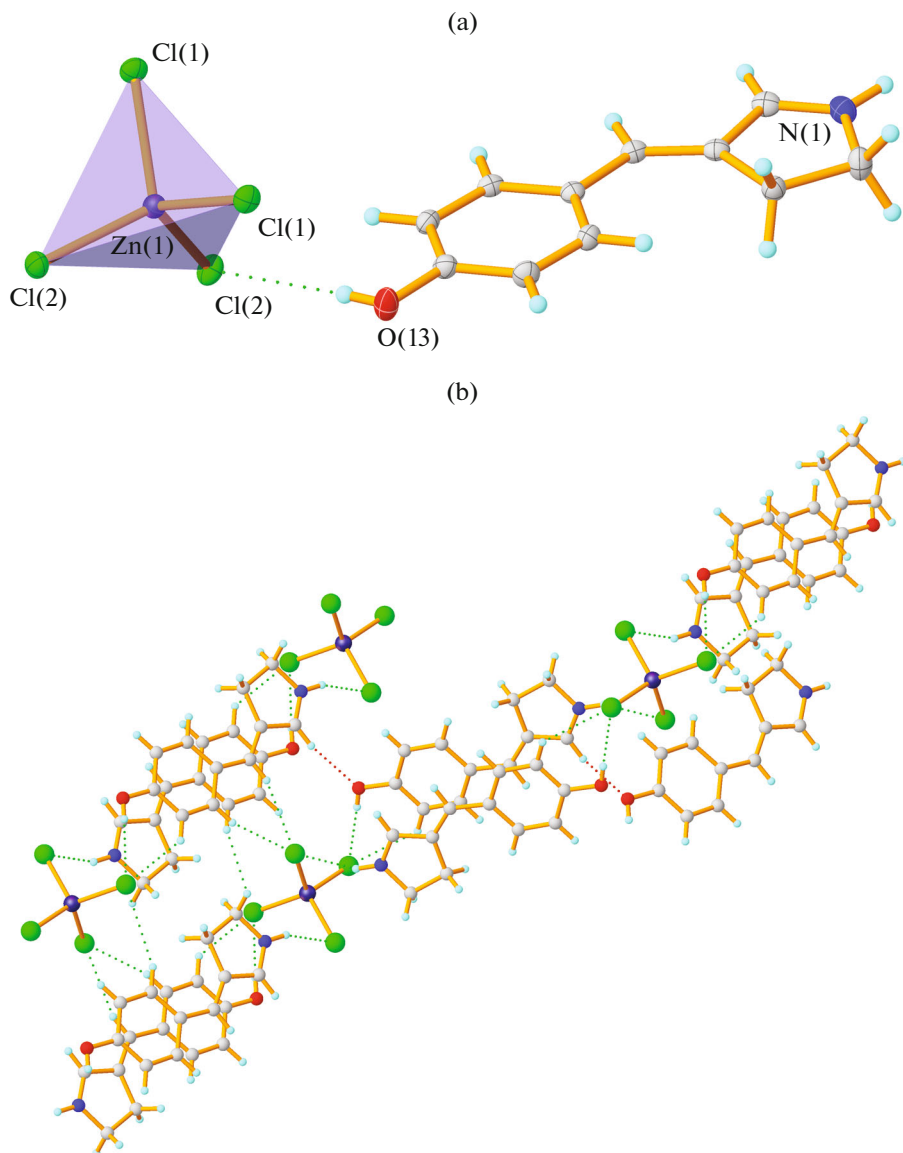


Fig. 4. (a) Structure of complex salt **IV** in the crystal; (b) fragment of the crystal packing of **IV**.

pounds described here and for organic pyrrolinium trifluoroacetates described earlier [25] demonstrates that the geometry of interactions is preserved irrespective of the anion nature. The only possible exception is the salt of iron tris-dimethylmalonate (**II**), in which the NHO angles are somewhat distorted (Table 3). However, this fact is easily explained by more sophisticated structure of the complex anion compared to the other anions and the larger number of other hydrogen-bonding sites, which results in a more complex system of hydrogen bonds in the crystal.

Thus, we described methods for the synthesis of five new complex salts of 3-arylidene-1-pyrrolinium derivatives, characterized the structure of these salts,

and identified the principal structural motifs of complex formation.

ACKNOWLEDGMENTS

X-ray diffraction analysis, IR spectroscopy, and C,H,N,S analysis were performed using equipment of the Center for Collective Use of Physical Investigation Methods of the Kurnakov Institute of General and Inorganic Chemistry, Russian Academy of Sciences, supported by the state assignment of the Kurnakov Institute of General and Inorganic Chemistry, Russian Academy of Sciences, in the field of fundamental research.

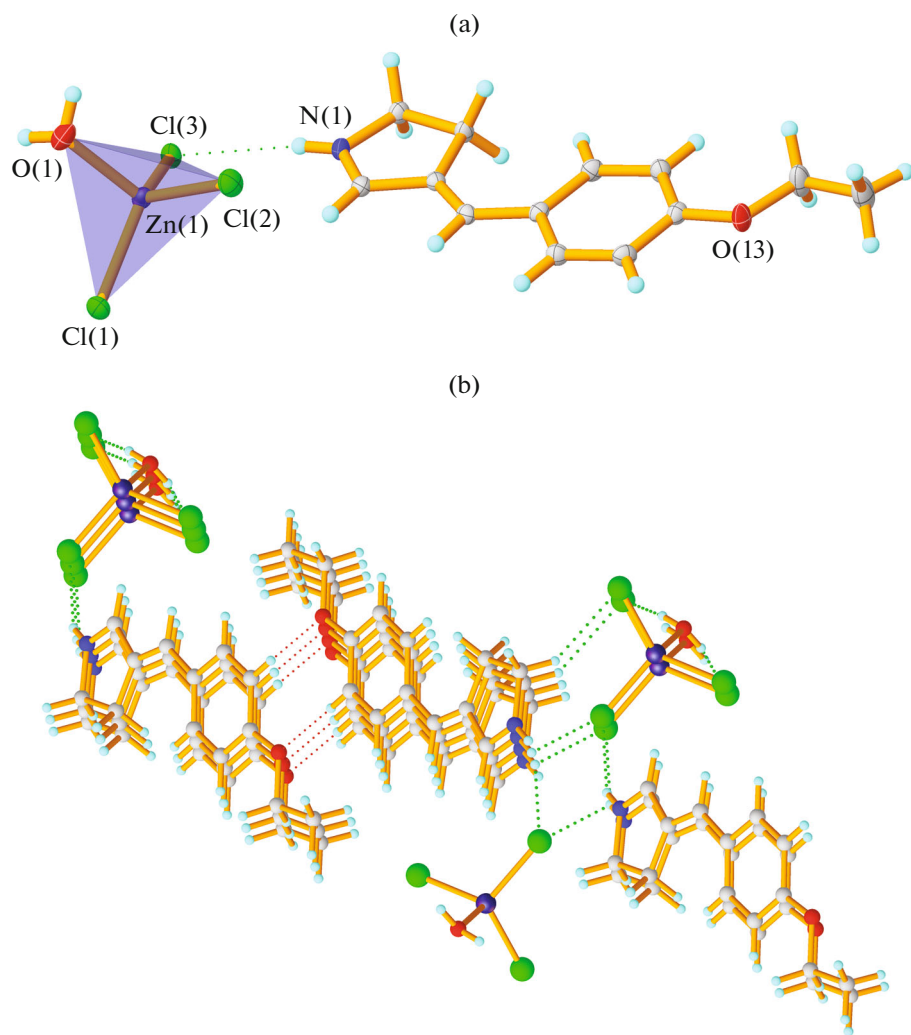


Fig. 5. (a) Structure of complex salt **V** in the crystal; (b) fragment of the infinite hydrogen-bonded chain in the crystal of **V**.

FUNDING

This study was supported by the Russian Science Foundation (project no. 21-73-00074).

CONFLICT OF INTEREST

The authors declare that they have no conflicts of interest.

REFERENCES

- Karunananda, M.K., Vazquez, F.X., Alp, E.E., et al., *Dalton Trans.*, 2014, vol. 43, p. 13661.
- Yeary, L.W., Moon, J.-W., Rawn, C.J., et al., *J. Magn. Magn.*, 2011, vol. 323, no. 23, p. 3043.
- Doungmene, F., Aparicio, P.A., Ntienoue, J., et al., *Electrochim. Acta*, 2014, vol. 125, p. 674.
- Reddy, T.S., Priver, S.H., Mirzadeh, N., et al., *Inorg. Chem.*, 2020, vol. 59, no. 8, p. 5662.
- Catto, M., Aliano, R., Carotti, A., et al., *Eur. J. Med. Chem.*, 2010, vol. 45, no. 4, p. 1359.
- Adonin, S.A., Gorokh, I.D., Samsonenko, D.G., et al., *Polyhedron*, 2019, vol. 159, p. 318.
- Gorokh, I.D., Adonin, S.A., Novikov, A.S., et al., *Polyhedron*, 2019, vol. 166, p. 137.
- Adonin, S.A., Gorokh, I.D., et al., *J. Struct. Chem.*, 2017, vol. 58, no. 4, p. 718.
- Adonin, S.A., Bondarenko, M.A., Abramov, P.A., et al., *Z. Anorg. Allg. Chem.*, 2019, vol. 645, nos. 18–19, p. 1141.
- Usol'tsev, A.N., Shentseva, I.A., Shayapov, V.R., et al., *Russ. J. Inorg. Chem.*, 2021, vol. 66, no. 10, p. 1482.
- Tyroller, S., Zwischenpflug, W., and Richter, E., *J. Agric. Food Chem.*, 2002, vol. 50, no. 17, p. 4909.
- Pluotno, A. and Carmeli, Sh., *Tetrahedron*, 2005, vol. 61, no. 3, p. 575.
- Laohakunjit, N. and Noomhorm, A., *Flavour Fragrance J.*, 2004, vol. 19, no. 3, p. 251.

14. Dannhardt, G. and Kiefer, W., *Arch. Pharm.*, 2001, vol. 334, no. 6, p. 183.
15. Klintworth, R., de Koning, Ch.B., Opatz, T., et al., *Org. Chem.*, 2019, vol. 84, no. 17, p. 11025.
16. Guillard, R., Kadish, K., Smith, K., et al., *The Porphyrin Handbook*, San Diego: Academic, 2003.
17. Micheletti, G., Delpivo, C., and Baccolini, Gr., *Green Chem. Lett. Rev.*, 2013, vol. 6, no. 2, p. 135.
18. Boga, C., Cino, S., Micheletti, G., et al., *Org. Biomol. Chem.*, 2016, vol. 14, no. 29, p. 7061.
19. Haria, M. and Balfour, J.A., *CNS Drugs*, 1997, vol. 7, no. 2, p. 159.
20. Gazizov, A.S., Smolobochkin, A.V., Burilov, A.R., et al., *Tetrahedron Lett.*, 2020, vol. 61, no. 39, p. 152371.
21. Smolobochkin, A.V., Melyashova, A.S., Gazizov, A.S., et al., *Russ. J. Org. Chem.*, 2020, vol. 56, p. 1115.
22. Melyashova, A.S., Smolobochkin, A.V., Gazizov, A.S., et al., *Tetrahedron*, 2019, vol. 75, no. 47, p. 130681.
23. Smolobochkin, A.V., Gazizov, A.S., Urgenishbay, N.M., et al., *Russ. Chem. Bull.*, 2020, vol. 69, no. 2, p. 382.
24. Smolobochkin, A.V., Melyashova, A.S., Gazizov, A.S., et al., *Russ. J. Gen. Chem.*, 2018, vol. 88, p. 1934.
25. Smolobochkin, A.V., Gazizov, A.S., Melyashova, A.S., et al., *RSC Advances*, 2017, vol. 7, no. 80, p. 50955.
26. Krause, L., Herbst-Irmer, R., Sheldrick, G.M., et al., *J. Appl. Crystallogr.*, 2015, vol. 48, p. 3.
27. Sheldrick, G.M., *Acta Crystallogr. Sect. A: Found. Adv.*, 2015, vol. 71, p. 3.
28. Sheldrick, G.M., *Acta Crystallogr. Sect. C: Cryst. Chem.*, vol. 71, p. 3.
29. Dolomanov, O.V., Bourhis, L.J., Gildea, R.J., et al., *J. Appl. Crystallogr.*, 2009, vol. 42, p. 339.
30. Llunell, M., Casanova, D., Cirena, J., et al., *SHAPE. Version 2.1. Program for the Stereochemical Analysis of Molecular Fragments by Means of Continuous Shape Measures and Associated Tools*, Barcelona: Universitat de Barcelona, 2013.
31. Clegg, W., *Acta Crystallogr. Sect. C: Cryst. Struct. Commun.*, 1985, vol. 41, p. 1164.
32. Calogero, S., Stievano, L., Diamandescu, L., et al., *Polyhedron*, 1997, vol. 16, no. 23, p. 3953.

Translated by Z. Svitankos